

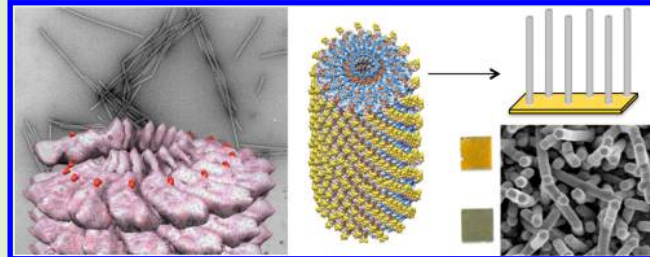
Carboxylate-Directed In Vivo Assembly of Virus-like Nanorods and Tubes for the Display of Functional Peptides and Residues

Adam D. Brown,^{†,‡,#} Lindsay Naves,^{†,#} Xiao Wang,[†] Reza Ghodssi,^{§,||} and James N. Culver*,^{†,⊥}

[†]Institute for Bioscience and Biotechnology Research, [‡]Fischell Department of Bioengineering, [§]Institute for Systems Research, ^{||}Department of Electrical and Computer Engineering, and [⊥]Department of Plant Science and Landscape Architecture, University of Maryland, College Park, Maryland 20742, United States

Supporting Information

ABSTRACT: Uniform dimensions and genetic tractability make filamentous viruses attractive templates for the display of functional groups used in materials science, sensor applications, and vaccine development. However, active virus replication and recombination often limit the usefulness of these viruses for such applications. To circumvent these limitations, genetic modifications of selected negatively charged intersubunit carboxylate residues within the coat protein of tobacco mosaic virus (TMV) were neutralized so as to stabilize the assembly of rod-shaped virus-like particles (VLPs) within bacterial expression systems. Here we show that TMV-VLP nanorods are easily purified, stable, and can be programmed in a variety of configurations to display functional peptides for antibody and small molecule binding.



INTRODUCTION

Virus particles are remarkable examples of biological evolution. They consist of individual components that encode the ability to self-assemble into uniform nanoscale shapes. These traits have made viruses attractive templates for use in nanotechnology applications. Furthermore, the protein and genetic components that make up these particles display a unique level of malleability that enables both genetic and chemical modifications for the addition of novel functionalities that include vaccine epitopes, moieties for the mineralization of inorganics, and genetics for the patterning of virus particles.^{1–4} Yet despite these traits, the application of virus particles is often limited by problems associated with viral replication and recombination that result in the loss of the desired functionalities. In addition, size constraints dictated by the need to include replication-competent virus genomes also reduce the potential application of these particles. However, many of these limitations can be circumvented by the use of virus-like particles (VLPs) derived from the assembly of virus structural proteins in the absence of the virus genome.^{1,5,6} Yet a number of virus coat proteins, filamentous viruses in particular, are not amenable to particle assembly in the absence of nucleic acid. Here we describe an *in vivo* VLP assembly system for the filamentous Tobacco mosaic virus (TMV) and its application for the display of functional binding residues and peptides.

TMV has served as a model virus for use in a variety of applications.⁷ TMV forms a nanotube structure 300 nm in length and 18 nm in diameter with a 4 nm diameter hollow inner channel. Each particle is assembled from ~2130 identical 17.5 kDa protein subunits wrapped in a helix around a single strand of plus strand viral RNA.⁸ TMV particles are stable up to

60 °C and at pH range of 2–10⁹ and are amenable to genetic modifications for the addition of novel functionalities that include inorganic binding and vaccine epitope display.^{7,10,11} Combined, these traits make the virus a durable biological template. However, the use of infectious TMV imparts limitations associated with virus recombination and replication.¹¹ In addition, *in planta* production of virus particles requires specialized plant growth conditions and produces an infectious particle. These limitations often result in the loss of genetically added sequences via recombination or the inability to generate sufficient quantities of virus particles due to interference in the virus life cycle by the added sequence or peptide.¹²

Previous studies have demonstrated that the TMV coat protein can be expressed and purified from *Escherichia coli*.^{13–15} However, at neutral pH, purified TMV coat proteins are only capable of assembling into lower order disk-shaped aggregates. Assembly of these aggregates into characteristic rod-shaped particles requires the coexpression of RNA containing the virus origin of assembly, leading to the production of VLPs containing nucleic acid.¹⁶ Alternatively, exposure of purified coat protein to pH 5 buffer conditions is also known to induce the formation of rod-shaped particles.¹⁷ Both of these approaches entail drawbacks that can limit the usefulness of the TMV coat protein generated VLPs. For example, recruitment to the bacterial polyribosomes can significantly disrupt the production of RNA assembled VLPs.¹⁸ Further-

Received: May 23, 2013

Revised: July 20, 2013

Published: July 24, 2013

more, the presence of nucleic acid within the rod may be undesirable for some applications. Assembly through post-purification pH treatments is also problematic in that neutral pH conditions necessary for many biological and chemical functions lead to the disassembly of these VLPs, thus limiting their use. New methods that permit the self-assembly of the TMV coat protein under biological relevant conditions are needed.

Stability of the TMV particle is modulated by repulsive carboxylate groups located on opposite sides of subunit-to-subunit interfaces.^{8,18} These negatively charged repulsive interactions are stabilized by protons and Ca²⁺ ions that function as a stability switch. Specifically, within the extracellular environment excess Ca²⁺ ions and protons function to negate repulsive carboxylate interactions, stabilizing the virus particle. However, lower Ca²⁺ ion concentrations and higher pH of the cellular environment results in the loss of stabilizing ions and protons, leading to particle disassembly and infection. Structural and mutational studies have identified three specific intersubunit carboxylate interactions within the TMV particle.^{8,19} One carboxylate interaction occurs between Asp116 and phosphate from the viral nucleic acid. Another forms a lateral cluster of interactions at the virion inner radius between E106 of one subunit and E95, E97, and D109 of the adjacent subunit. The third occurs axial between residues E50 and D77 (Figure 1A). The E50–D77 interaction has been

and develop an *in vivo* TMV VLP assembly system for the patterning and display of functional residues and peptides.

METHODS SECTION

TMV Coat Protein Expression Constructs. The TMV coat protein open reading frame (ORF) carrying the E50Q and D77N modifications was codon optimized for expression in *E. coli* (GenScript, Piscataway NJ; Supporting Information) and inserted into the pET-21a(+) expression vector (Novagen, Madison WI) via *Nde*I and *Xho*I restriction sites. Further modifications to the N- and C-terminus of the coat protein ORF were achieved by primer-based polymerase chain reaction (PCR) mutagenesis using oligonucleotides containing additional or altered sequences (Table 1). A cysteine codon was added at position two at the N-terminus of the coat protein ORF to produce TMV-VLP1cys for enhanced metal coatings and oriented surface-binding.²¹ Sequences encoding the binding peptides for the FLAG epitope (DYKDDDDK) were added to the coat protein C-terminus.²² Sequences binding the fluorescent imaging agent Genhance 680 (IQSPHFF) were added to the coat protein C-terminus as fusions either with or without preceding sequences encoding a “leaky” amber stop codon (TAG) or a flexible 10 amino acid linker (GGGGSGGGGS).^{23,24} Amplified PCR products containing 5' *Nde*I and 3' *Xho*I restriction sites were used to ligate the modified coat protein ORFs into similarly cut pET-21a(+) vector.

Induction and Purification of TMV-VLPs. Coat protein expression constructs were transformed into BL21 competent *E. coli* K-12. Additionally, JM109 *E. coli* cells were used for coat protein constructs containing the amber stop codon TAG. JM109 cells carry the supE44 suppressor of the amber stop codon via a tRNA mutation that transitions the GUC glutamine anticodon to AUC.²⁵ Transformed cells were cultured at 37 °C in LB broth containing ampicillin (100 µg/mL)/chloramphenicol (50 µg/mL) for BL21 and ampicillin (100 µg/mL)/nalidixic acid (30 µg/mL) for JM109 cells to an OD₆₀₀ of 0.5. Cells were then induced by the addition of 0.1 mM IPTG and incubated overnight at 25 °C. Induced cells were harvested by centrifugation at 4 °C and lysed using Bugbuster with Lysonase according to the manufacturer's protocol (Novagen, Madison WI). Dithiothreitol to a concentration of 0.5 mM was added to the cell lysates followed by 3–5 min of sonication in a Branson 1510 sonicator (Branson Ultrasonics, Danbury CT). One third volume of chloroform was then added to the lysates, mixed and separated by centrifugation for 10 min at 17,000 × g at 4 °C. Because of the hydrophobic nature of the IQ peptide the chloroform purification step was replaced by centrifugation at 800 × g for 1 min, centrifugation of the resulting supernatant at 66 400 × g for 30 min, and resuspension of the pellet in 3 mL of 0.1 M pH 7 sodium phosphate buffer. VLPs were then precipitated by the per volume addition of 1.5% KCl and 6% polyethylene glycol for 1 h at 4 °C. VLPs were then pelleted by centrifugation for 10 min at 17 000 × g. The resulting pellet was resuspended by shaking overnight in 0.5 to 2 mL of 0.1 M pH 7 sodium phosphate buffer. Resuspended VLP pellets were then loaded onto a 10 to 40% sucrose gradient in 0.1 M pH 7.0 sodium phosphate buffer and centrifuged for 1 h at 91 000 × g at 14 °C. A diffuse band corresponding to the purified VLP was removed by syringe and concentrated by centrifugation for 1 h at 92 000 × g at 4 °C. The purified VLP pellet was then resuspended in 0.1 M pH 7 sodium phosphate buffer.

To visualize VLPs within bacteria, cells were induced overnight and subsequently prepared by pelleting, followed by fixing in 2%

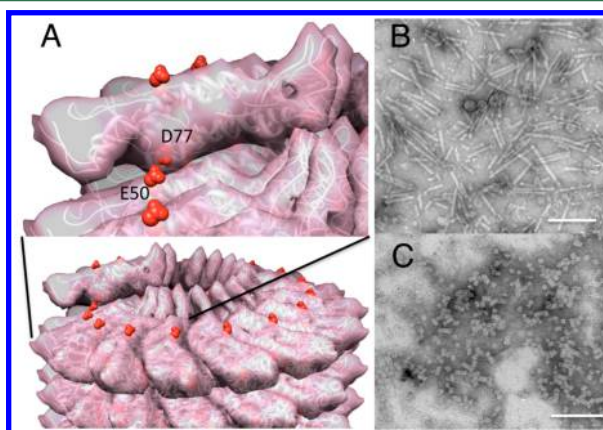


Figure 1. Carboxylate modifications to the TMV coat protein promote particle assembly. (A) Molecular model of the rod surface showing the location of the juxtaposed E50–D77 carboxylate pair. (B) Electron micrograph of crude bacterial lysates derived from the expression of the E50Q/D77N coat protein ORF. (C) Electron micrograph of crude bacterial lysates from the unmodified coat protein showing only disks and short stacks of disks. Bars equal 200 nm.

shown to be a significant driver in helical rod assembly as mutations E50Q and D77N have been shown to block virus disassembly and produce empty virus-like helical rods during infection.^{18–20} We have exploited these findings to investigate

Table 1. Primer Sequences for TMV-VLP Constructs

primer	sequence
N-term. 1cys	5'-GGCATATGTCGTGTTAGCATTACCACCCCG-3'
C-term. FLAG	5'-GCTCGAGTTACTTGTATCGTCATCTTGTAATC GGTTGCCGGACCAGAGGT-3'
C-term. leaky amber stop + IQ-tag	5'-GCTCGAGTTAGAAGAAATGCGGAGACTGAATC TAGGTTGCCGGACCAGAGGT-3'
C-term. leaky amber stop + flexible linker + IQ-tag	5'-GCTCGAGTTAGAAGAAATGCGGAGACTGAATA CTGCCTCCACCGCCGCTGCCACCTCCGCCCTAGGTTGCCGGACCAGAGGT-3'

glutaraldehyde in phosphate buffered saline (PBS) with 0.29 M sucrose. Postfixing was done in en bloc on the pelleted cells using 1% osmium tetroxide with 2% aqueous uranyl acetate. Dehydration of the pelleted cells was accomplished by treatment with solutions of increasing ethanol content (100% final). The dehydrated pellet was then embedding by solutions of propylene oxide with increasing Spurr's resin content (100% final) and curing at 70 °C overnight. Expressed VLPs were visualized in whole fixed bacterial cells and in purified form using a transmission electron microscope at 80 kV.

VLP Surface Assembly and Electroless Plating. Purified TMV-VLP1cys was self-assembled onto 1 cm² gold-coated silicon chips by incubation overnight at 4 °C in a 1 mg/mL solution of the purified VLPs resuspended in 0.1 mM sodium phosphate buffer, pH 7. VLP assembled chips were then dipped in a 0.158 mM solution of Na₂PdCl₄ for 30 min at 4 °C. The surface-bound VLPs were then coated with nickel by moving the chip directly into an electroless nickel plating solution consisting of 0.05 M NiCl₂, 0.12 M glycine, 0.0785 M sodium tetraborate, 0.525 M dimethylamine borane complex at pH 7. Nickel deposition by reduction was allowed to proceed at room temperature until the entire surface of the chip had darkened. Nickel coatings were visualized via field emission electron microscopy.

Chip-Based Enzyme-Linked Immunosorbent Assay (ELISA). Gold-coated 1 cm² silicon nitrate chips were submerged overnight in purified TMV1cys-VLP or TMV1cys-VLP1cys-FLAG at 4 °C to facilitate oriented VLP assembly onto the gold surface. VLP assembled chips were then incubated for an additional 30 min at 4 °C in Tris buffered saline (TBS; 50 mM Tris-HCl, 200 mM NaCl) pH 7.0 containing 5% nonfat dry milk as a blocking agent. Chips were then rinsed three times by submersion in fresh TBS buffer. Rinsed chips were subsequently incubated for 3 h at room temperature in TBS containing 5% nonfat dry milk and a 1/1000 dilution of rabbit anti-flag antibody (Sigma-Aldrich, St. Louis MO). The chip was then rinsed three times with TBS buffer and twice with TBS buffer containing 0.05% Tween-20. After rinsing, chips were submerged in TBS with 5% nonfat dry milk containing a 1/5000 dilution of antirabbit IgG alkaline phosphatase and incubated at room temperature for 3 h. Chips were again rinsed as described above and placed directly in a solution containing 0.15 mg/mL of 5-bromo-4-chloro-3-indoyl phosphate and 0.3 mg/mL NitroBT in substrate buffer (10 mM Tris-HCl pH 9.5, 100 mM NaCl and 5 mM MgCl₂-6H₂O) and incubated for 10 min at room temperature. The reaction was stopped by immersion in water and the chips dried. Color intensities of individual chips were measured using ImageJ software.²⁶

Fluorescence Binding onto IQ Peptide Tagged TMV-VLPs. The IQ-tag modified VLPs were tested for preferential binding of the fluorescent imaging agent Genhance 680 (PerkinElmer, Waltham MA) as follows. Purified TMV1cys-VLP-AmberFlex-IQ (0.2 mg/mL or 0.02 mg/mL) were incubated overnight at 4 °C in 0.5 mL of 0.1 M pH 7 phosphate buffer with or without the addition of 10 μL of 0.1 mg/mL Genhance 680. Samples were then centrifuged at 16 000 × g for 45 min. The VLP pellets were then resuspended in 1 mL of 0.1 M pH 7.0 phosphate buffer and centrifuged again for 45 min. Pelleted VLPs were then resuspended in 0.1 M pH 7.0 phosphate buffer to a concentration of 0.5 mg/mL and 0.05 mg/mL. Two hundred microliters of each sample was added to a black-walled 96-well microtiter plate, and fluorescence intensity at 690 nm (655 nm excitation and a 665 nm cutoff) was determined using a SpectraMax M2 (Molecular Devices, Sunnyvale, CA).

RESULTS

Expression and Characterization of Modified TMV Coat Protein VLPs. The TMV coat protein open reading frame was codon optimized for prokaryotic expression and synthesized either with or without E50Q and D77N substitutions (See Supporting Information). Bacterial expression of the modified coat protein open reading frames was achieved via IPTG inducible bacterial expression vectors. Induced bacterial cultures were lysed, and the crude extracts

were analyzed for TMV coat protein expression and assembly. Polyacrylamide gel electrophoresis (PAGE) analysis of bacterial lysate demonstrated coat protein expression (Figure 2A, lane

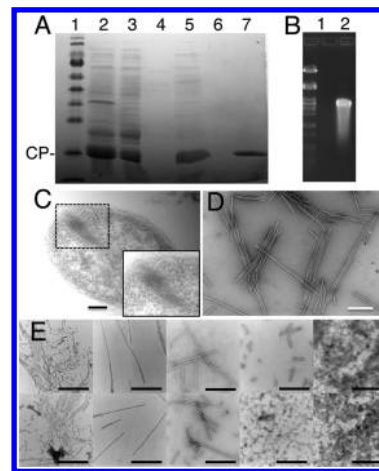


Figure 2. Expression and purification of TMV-VLPs from *E. coli* extracts. (A) PAGE analysis of VLP purification scheme. Lane 1, protein marker; lane 2, lysed extract from IPTG induced bacteria; lane 3, chloroform clarified extract; lane 4, supernatant from PEG precipitation; lane 5, pellet from the PEG precipitation; lane 6, supernatant from the sucrose fractionation; lane 7, pellet from the sucrose fractionation. (B) Agarose gel electrophoresis of RNA extracts from purified TMV-VLPs (Lane 1) and TMV virions (Lane 2). Band in lane 2 represents the TMV genome. (C) Thin section electron micrograph of a fixed *E. coli* cell showing the presence of assembled TMV-VLPs. D, Purified TMV-VLPs from the sucrose gradient resuspended pellet. Bars equal 200 nm. (E) Transmission electron microscope images of TMV1cys (top row) and TMV1cys-VLP (bottom row) adjusted to pH 3, 5, 7, 9, and 11 (left to right). Bars equal 500 nm.

2). Electron microscopy demonstrated the presence of rod-shaped VLPs consistent with the helical assembly of the TMV coat protein (Figure 1B). In contrast, the unmodified wild-type optimized TMV coat protein ORF produced only disks and stacks of disks when similarly expressed (Figure 1C). Subsequent thin section electron microscopy of induced bacterial cells also displayed the presence of rod-shaped TMV-like particles within the bacterial cells (Figure 2C).

Purification of these particles was easily accomplished via sucrose gradient centrifugation of chloroform cleared bacterial extracts. PAGE analysis from each purification step (bacterial lysate, chloroform clarification, PEG precipitation and sucrose gradient fractionation) shows the selective purification of the VLPs (Figure 2A, lanes 3–6) while electron microscopy of the final gradient fractions (Figure 2A, lane 7) shows the purity of the VLPs (Figure 2D). Concentrations of purified rod-shaped VLPs of over 70 mg per liter of culture were routinely obtained using this method. An analysis of purified particles indicated a width (18 nm) and inner channel size (4 nm) consistent with the virus particle. However, the length of the bacterial purified particles was highly variable with many particles substantially longer than the 300 nm virus produced particles (Figure 2D). Variable VLP lengths indicate an absence of RNA, which typically controls virus particle length. Subsequent nucleic acid extractions from purified VLPs confirmed the lack of nucleic acid in these particles (Figure 2B, lane 1). By contrast, similar nucleic acid extractions from purified virus samples produced an abundant amount of genomic viral RNA (Figure 2B, lane 2).

Combined these findings demonstrate that the E50Q/D77N mutations are sufficient to drive the nucleic acid free assembly of the TMV coat protein within the bacterial expression system.

To compare the relative pH-dependent stability of TMV virions to TMV-VLP rods, samples were exposed to a pH range of 3–11. One hundred microliters of 1 mg/mL TMV1cys and TMV1cys-VLP in 0.1 M pH 7 phosphate buffer was first dialyzed against 200 mL 0.1 M pH 7 Tris. The samples were then divided and dialyzed against 200 mL 0.1 M Tris adjusted to pH 3, 5, 7, 9, or 11 for 72 h. The resulting suspensions were examined by transmission electron microscopy. The results showed a similar stability profile for TMV1cys-VLP as compared to RNA-containing virus rods (Figure 2E). Both were shown to be stable at pH 5 and 7, with longer rods present at pH 5, and both exhibited fracturing of rods at pH 3 and 9. Both samples at pH 11 showed complete loss of visible structure.

Surface Attachment and Inorganic Coatings of TMV1cys-VLPs. To examine the stability of the bacterial assembled TMV-VLPs, we assessed their ability to be surface assembled and metal coated. Previous studies using the TMV1cys virus have demonstrated a robust ability of this virus to bind surfaces in an oriented fashion (from one end of the rod) and via electroless plating produce uniform metal coatings.^{21,27} The positioning of the N-terminus 1cys mutation directs the attachment and vertical positioning of the viral rod-shaped particles onto gold, steel, or other metal surfaces.²¹ Although surface exposed, the 1cys mutation is recessed within a groove and partially covered by the C-terminal arm of the coat protein. This position inhibits direct contact between the cysteine derived thiol and metal surfaces except at the 3' end of the virion rod where the thiol group is sufficiently exposed to make direct contact with the gold surface (Figure 3A). Here we

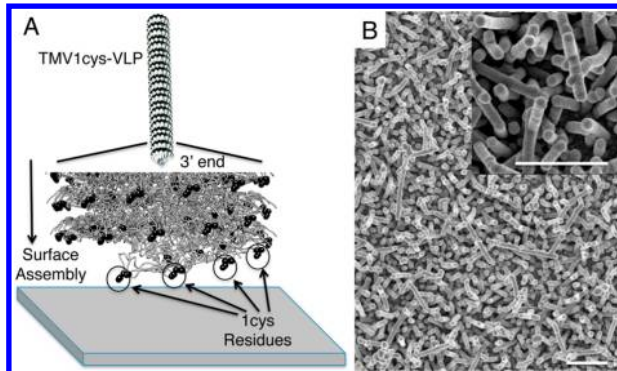


Figure 3. Surface binding and electroless plating of TMV1cys-VLPs. (A) Molecular models showing the location and binding of the TMV1cys-VLP modification for the oriented attachment of the VLPs onto a gold coated surface. (B) Scanning electron micrograph of a TMV1cys-VLP assembled surface electroplated with nickel. Bars equal 1 μ m.

show that the addition of the 1cys mutations to the E50Q/D77N TMV-VLP ORF produces rod-shaped nanoparticles that readily assemble onto surfaces and can be easily metal coated using established electroless plating methods (Figure 3B).²¹ These findings demonstrate that even in the absence of viral RNA the E50Q–D77N VLP rods maintain robust stability during the extensive processing required for surface attachment and metallization.

Chip-Based ELISA. To examine the flexibility of the TMV-VLP assemblies we produced a set of modified coat protein ORFs for the display of peptides along the outer surface of the virus particle (Figure 4). The simplest system directly fused the

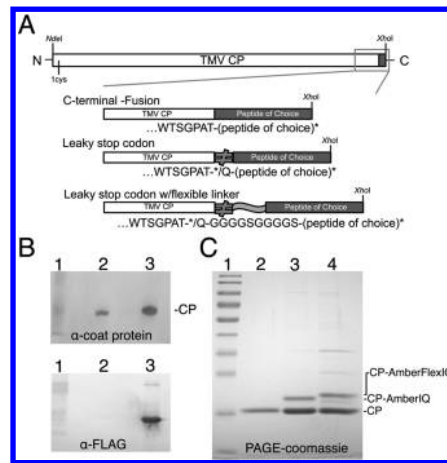


Figure 4. TMV-VLP expression constructs. (A) Diagram of TMV ORF with three variations for the expression and display of functional peptides. (B) Western blot analysis of purified TMV1cys-VLP-FLAG particles with either anticoat protein and anti-FLAG antibody. Lane 1, marker proteins; lane 2, the unmodified TMV1cys-VLP; lane 3, TMV1cys-VLP-FLAG. (C) PAGE analysis of purified TMV1cys-VLP-AmberIQ and -AmberFlexIQ constructs. Lane 1, marker proteins; lane 2, the unmodified TMV1cys-VLP; lane 3, TMV1cys-VLP-AmberIQ; lane 4, TMV1cys-VLP-AmberFlexIQ.

peptide of interest to the C-terminus coat protein ORF so that each coat protein subunit displays the desired peptide (Figure 4A,B). For these experiments, the eight amino acid FLAG peptide (DYKDDDDK) was fused directly to the C-terminal arm of the 1cys coat protein ORF to produce TMV1cys-VLP-FLAG. To examine the ability of TMV1cys-VLP-FLAG assembled peptides to bind their target molecules, we utilized a microchip based ELISA strategy for SiN chips.²⁸ TMV1cys-VLP-FLAG peptides were self-assembled onto gold coated chips and washed with PBS buffer to remove any excess unbound virus and blocked with 5% nonfat milk to reduce background. Incubation with anti-FLAG antibody and subsequent detection via an alkaline phosphatase linked anti-antibody produced a clear color precipitant with an antibody detection limit of $<10^{-6}$ mg/mL (Figure 5). Control chips assembled with TMV1cys-VLP without the FLAG peptide did not show detectable color changes. These studies demonstrate the utility of the TMV1cys-VLP system for the display and surface assembly of target peptides for detection purposes.

Controlled Peptide Display for VLP Assembly Small Molecule Detection. To further investigate the ability of the TMV-VLP system to function as a nanoscaffold for the display of functional peptides, we engineered the rod-shaped VLPs to display a seven amino acid “IQ” peptide (IQSPHFF) previously identified by phage display for its ability to bind the fluorescent imaging molecule Genhance 680.²⁴ However, initial attempts to purify TMV1cys-VLP rods with the IQ peptide fused directly to the C-terminus of the coat protein ORF failed (data not shown). We speculate that unlike the FLAG peptide, the IQ peptide produces misfolding of the coat protein and/or disrupts VLP rod assembly, possibly via steric hindrance between the stacked coat protein subunits. To circumvent these potential

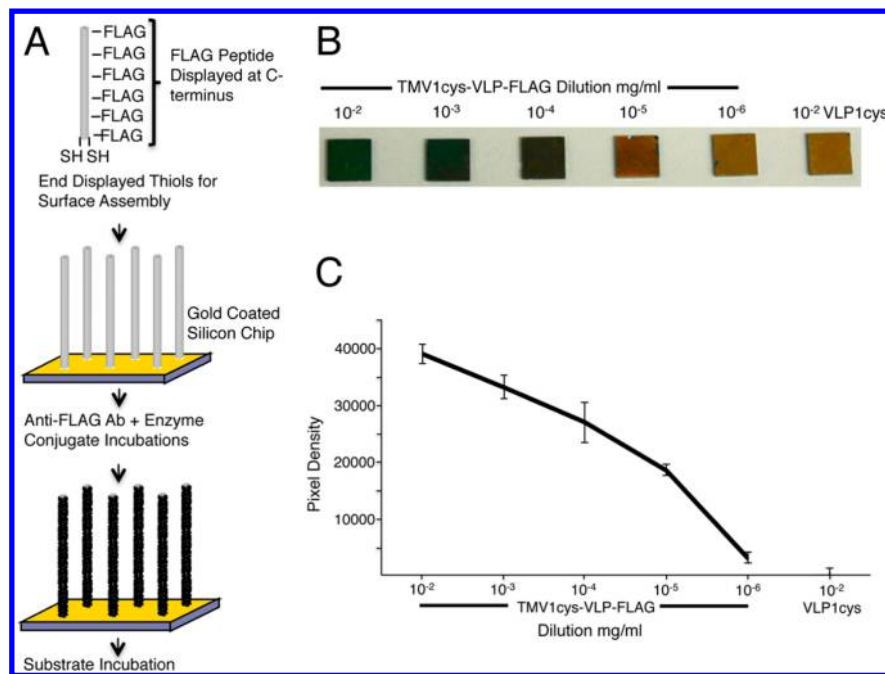


Figure 5. Use of TMV1cys-VLPs in a chip-based ELISA detection system. (A) Diagram of VLP assembly and detection system. (B) Gold-coated chips assembled with a range of TMV1cys-VLP-FLAG concentrations and processed as outlined in A. Note, the control chip coated with the 10⁻² mg/mL unmodified TMV1cys-VLP did not produce a substrate reaction after ELISA processing. (C) Density analysis of ELISA chips shown in B.

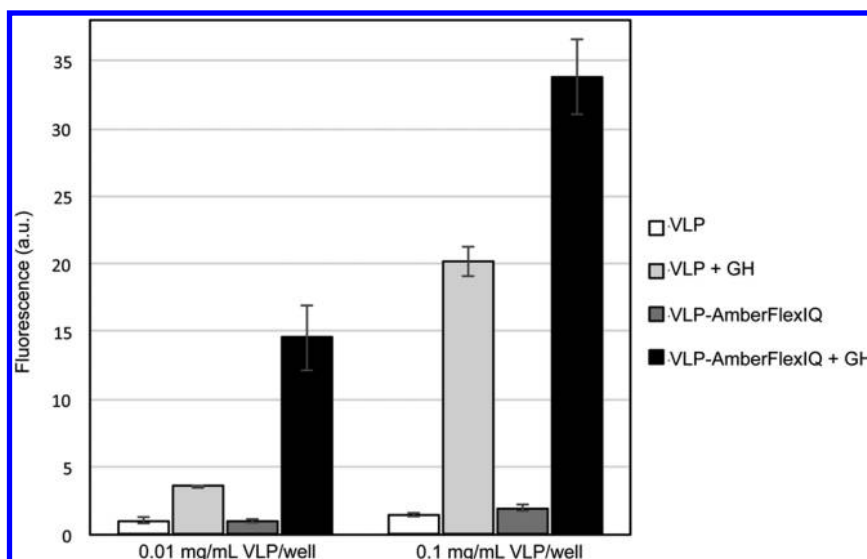


Figure 6. TMV-VLP directed binding of a fluorescent imaging agent. Purified TMV-VLPs at defined concentrations were mixed with Genhance 680 (GH) washed and assayed for fluorescence retention. Data is shown for the unmodified TMV-VLP (VLP) and TMV-VLP-AmberFlexIQ (VLP-AmberFlexIQ) both with and without GH treatment. Results show averaged \pm standard deviation from three assays.

problems an amber stop codon was added to the 3' end (C-terminus) of the coat protein ORF (Figure 4A). Expression of the amber stop construct from within the bacterial supE44 suppressor system directs the occasional incorporation of a glutamine residue at the TAG stop codon due to a tRNA mutation. This produces a mixture of coat proteins both with and without the additional peptide. A second construct adding a 10 amino acid flexible linker "Flex" (GGGGSGGGGS) in front of the IQ peptide was also created as a means to further reduce any interference the IQ peptide may have on VLP rod assembly (Figure 4A). The small side chains of this linker produce a highly flexible peptide sequence that has been used extensively for bridging functional peptide domains.²³ Bacterial

expression and subsequent VLP rod purifications produced significant quantities of these VLPs (Figure 4C). In particular, the TMV1cys-VLP construct expressing the amber stop with flexible linker produced nearly twice the concentration of purified VLPs, ~16 mg/L, in comparison to the construct with only the amber stop, ~9 mg/L. For both constructs, an average ~34% of the subunits derived from the purified VLP nanorods were read-through products of the amber stop codon and displayed the additional peptide sequences (Figure 4C, lanes 3 and 4). The ability to vary the expression and display of the desired peptide provides a means to significantly reduce disruptions in VLP assembly conferred by the desired peptide.

The ability of the TMV1cys-VLP displayed IQ peptides to bind their target analyte was also investigated. Purified TMV1cys-VLP-AmberFlexIQ scaffolds were mixed with Genhance 680, washed, and analyzed for retention of the fluorescent imaging agent. Results for the tested VLP concentrations indicate that the VLPs alone are capable of binding low levels of the fluorescent analyte in a nonspecific manner (Figure 6). However, addition of the IQ peptide sequence, creating TMV1cys-VLP-AmberFlexIQ, produced a significant increase in retained fluorescence over the unmodified control TMV1cys-VLP (Figure 6). This finding indicates that the IQ peptide maintains the ability to bind its target molecule when displayed from the TMV1cys-VLP-AmberFlexIQ scaffold.

■ DISCUSSION

In this study, the known structure and assembly mechanism of TMV was used to engineer a novel *in vivo* VLP assembly system. In nature, TMV occurs as a soilborne virus and has evolved a sensitive sensing system that allows the rod-shaped particle to remain stable in the soil environment yet become unstable upon entry into a host cell. This sensing system is controlled by juxtaposed carboxylate interactions that exist between subunits.^{8,18} These repulsive carboxylate interactions represent a key factor in virion assembly and disassembly. Removal of these interactions strengthens the association of the coat protein subunits through existing hydrophobic and salt bridge interactions, significantly stabilizing the helical rod assembly.²⁰ Carboxylate alterations E50Q and D77N significantly shift the coat protein assembly equilibrium toward the production of rod-shaped particles, thus driving helical rod assembly even in the absence of the viral RNA. This modification permits the production of rod-shaped TMV-VLPs from a simple *E. coli* expression system and greatly expands the potential usefulness of these biomacromolecules in a number of nanotechnology related applications.

Significantly, the ability to rapidly produce quantities of TMV nanorod VLPs directly from bacterial cultures greatly simplifies methods for the construction and purification of highly modified versions of these macromolecules. The use of this system eliminates problems such as recombination and reduced virus accumulations that can occur when the infectious virus functions as the template for the display of functional peptides and groups. Additionally, specialized plant growth facilities are not needed, making these macromolecules more accessible for use in a wider range of research settings. Furthermore, findings indicate that bacterially expressed TMV-VLPs display a similar level of stability and functionality as the plant produced viruses, including pH sensitivity, surface assembly, mineralization and sensor functions. Thus, stability conferred by the genetic neutralization of repulsive carboxylate groups is sufficient to produce robust VLP assemblies.

For virus particles, two areas of application that have been studied extensively are their use in materials fabrication and their ability to display functional groups for sensor or vaccine applications. Filamentous viruses including TMV and M13 have been developed as biotemplates for the deposition of a variety of inorganic materials.^{4,7} The rigidity of the TMV rod-shaped particle as well as its polar ends allows for the particle to be attached to a surface in vertical orientation, producing three-dimensional nanofeatured substrates that significantly improve electrode function in a variety of electrode chemistries.⁷ Similarly, TMV particles and coat protein have been genetically

engineered to display epitopes from a variety of agents including the malaria parasite, foot and mouth disease virus, and influenza A as a means to rapidly produce vaccine components.^{29–31} Findings from this study clearly indicate that the TMV-VLPs are similarly capable of functioning as biotemplates for inorganic coatings as well as nanoparticles for the display of functional epitopes.

The use of bacterial phage and related systems to display and screen peptide libraries is a powerful combinatorial technology for the identification of unique peptides that confer selective binding abilities.³² To date, phage display methods have been employed to identify numerous single chain antibodies as well as receptor peptides that bind various pathogens and toxins of importance, including heavy metals such as cadmium; toxins such as ricin, botulinum, shiga, and staphylococcal enterotoxin B; and bacterial pathogens including *E. coli* O157:H7.^{33–38} Many of these receptor peptides display binding affinities in the nanomolar range and are capable of detecting their target molecules in traditional ELISA systems at the nanogram level.^{24,39} However, a considerable gap between the identification of these receptor peptides and their assembly into functional devices remains. The TMV1cys-VLP based display system represents a simple means to genetically produce these peptides in a variety of configurations and in a nanostructured format that can be patterned three dimensionally onto a variety of surfaces. Combined, these attributes make this VLP system a powerful means for the controlled display of functional peptides.

■ CONCLUSION

We report here the development of a TMV-VLP display system that directs the *in vivo* production of virus-like nanorods and tubes from a simple bacterial expression system. This system is genetically tractable and produces stable rod-shaped VLPs that can be used to display functional groups and peptides in multiple configurations with potential applications in sensor, electrode, and therapeutics development. This VLP system greatly simplifies the production of these rod-shaped particles, eliminating the need to produce a full-length infectious clone of the virus for production in plants. This simple, genetically tractable system for the production of TMV based nanoparticles should provide greater accessibility for a wider core of researchers interested in utilizing these particles to address a variety of questions and applications.

■ ASSOCIATED CONTENT

Supporting Information

Nucleotide and protein sequence of the bacterial expressed TMV coat protein is provided in the Supporting Information. This material is available free of charge via the Internet at <http://pubs.acs.org>.

■ AUTHOR INFORMATION

Corresponding Author

*E-mail: jculver@umd.edu; Tel +1-301-405-2912.

Author Contributions

#These authors contributed equally.

Author Contributions

The manuscript was written through contributions of all authors. All authors have given approval to the final version of the manuscript.

Notes

The authors declare no competing financial interest.

ACKNOWLEDGMENTS

We wish to thank Tim Maugel in the Laboratory of Biological Ultrastructure at the University of Maryland, College Park, for assistance with EM imaging and sample fixation. This work was supported by Biochemistry Program of the Army Research Office award W911NF1110138 and Maryland Agricultural Experiment Station award MD-PSLA-0275.

REFERENCES

- (1) Saunders, K.; Lomonosoff, G. P. Exploiting plant virus-derived components to achieve in planta expression and for templates for synthetic biology applications. *New Phytol.* **2013**, DOI: 10.1111/nph.12204.
- (2) Liu, Z.; Qiao, J.; Niu, Z.; Wang, Q. Natural supramolecular building blocks: From virus coat proteins to viral nanoparticles. *Chem. Soc. Rev.* **2012**, *41* (18), 6178–94.
- (3) Pokorski, J. K.; Steinmetz, N. F. The art of engineering viral nanoparticles. *Mol. Pharm.* **2011**, *8* (1), 29–43.
- (4) Flynn, C. E.; Lee, S. W.; Peelle, B. R.; Belcher, A. M. Viruses as vehicles for growth, organization and assembly of materials. *Acta Mater.* **2003**, *51* (19), 5867–5880.
- (5) Yildiz, I.; Shukla, S.; Steinmetz, N. F. Applications of viral nanoparticles in medicine. *Curr. Opin. Biotechnol.* **2011**, *22* (6), 901–8.
- (6) Dedeo, M. T.; Finley, D. T.; Francis, M. B. Viral capsids as self-assembling templates for new materials. *Prog. Mol. Biol. Transl. Sci.* **2011**, *103*, 353–92.
- (7) Lee, S. Y.; Lim, J. S.; Harris, M. T. Synthesis and application of virus-based hybrid nanomaterials. *Biotechnol. Bioeng.* **2012**, *109* (1), 16–30.
- (8) Namba, K.; Pattanayek, R.; Stubbs, G. Visualization of protein–nucleic acid interactions in a virus-refined structure of intact tobacco mosaic virus at 2.9 Å resolution by X-ray fiber diffraction. *J. Mol. Biol.* **1989**, *208* (2), 307–325.
- (9) Stubbs, G. Molecular structures of viruses from the tobacco mosaic virus group. *Semin. Virol.* **1990**, *1*, 405–412.
- (10) Smith, M. L.; Fitzmaurice, W. P.; Turpen, T. H.; Palmer, K. E. Display of peptides on the surface of tobacco mosaic virus particles. *Curr. Top. Microbiol. Immunol.* **2009**, *332*, 13–31.
- (11) Yusibov, V.; Shivprasad, S.; Turpen, T. H.; Dawson, W.; Koprowski, H. Plant viral vectors based on tobamoviruses. *Curr. Top. Microbiol. Immunol.* **1999**, *240*, 81–94.
- (12) Rabindran, S.; Dawson, W. O. Assessment of recombinants that arise from the use of a TMV-based transient expression vector. *Virology* **2001**, *284* (2), 182–9.
- (13) Hwang, D. J.; Roberts, I. M.; Wilson, T. M. Assembly of tobacco mosaic virus and TMV-like pseudovirus particles in *Escherichia coli*. *Arch. Virol. Suppl.* **1994**, *9*, 543–58.
- (14) Dedeo, M. T.; Duderstadt, K. E.; Berger, J. M.; Francis, M. B. Nanoscale protein assemblies from a circular permutant of the tobacco mosaic virus. *Nano Lett.* **2010**, *10* (1), 181–6.
- (15) Bruckman, M. A.; Soto, C. M.; McDowell, H.; Liu, J. L.; Ratna, B. R.; Korpany, K. V.; Zahr, O. K.; Blum, A. S. Role of hexahistidine in directed nanoassemblies of tobacco mosaic virus coat protein. *ACS Nano* **2011**, *5* (3), 1606–16.
- (16) Hwang, D. J.; Roberts, I. M.; Wilson, T. M. Expression of tobacco mosaic virus coat protein and assembly of pseudovirus particles in *Escherichia coli*. *Proc. Natl. Acad. Sci. U.S.A.* **1994**, *91* (19), 9067–71.
- (17) Durham, A.; Finch, J.; Klug, A. States of aggregation of tobacco mosaic virus. *Nature* **1971**, *229*, 37–42.
- (18) Culver, J. N.; Dawson, W. O.; Plonk, K.; Stubbs, G. Site-Directed Mutagenesis Confirms the Involvement of Carboxylate Groups in the Disassembly of Tobacco Mosaic-Virus. *Virology* **1995**, *206* (1), 724–730.
- (19) Lu, B.; Stubbs, G.; Culver, J. N. Carboxylate interactions involved in the disassembly of tobacco mosaic tobamovirus. *Virology* **1996**, *225* (1), 11–20.
- (20) Lu, B.; Taraporewala, Z. F.; Stubbs, G.; Culver, J. N. Intersubunit interactions allowing a carboxylate mutant coat protein to inhibit tobamovirus disassembly. *Virology* **1998**, *244* (1), 13–19.
- (21) Royston, E.; Ghosh, A.; Kofinas, P.; Harris, M. T.; Culver, J. N. Self-assembly of virus-structured high surface area nanomaterials and their application as battery electrodes. *Langmuir* **2008**, *24* (3), 906–912.
- (22) Einhauer, A.; Jungbauer, A. The FLAG peptide, a versatile fusion tag for the purification of recombinant proteins. *J. Biochem. Biophys. Methods* **2001**, *49* (1–3), 455–65.
- (23) Lu, P.; Feng, M. G. Bifunctional enhancement of a β-glucanase-xylanase fusion enzyme by optimization of peptide linkers. *Appl. Microbiol. Biotechnol.* **2008**, *79* (4), 579–87.
- (24) Kelly, K. A.; Carson, J.; McCarthy, J. R.; Weissleder, R. Novel peptide sequence (“IQ-tag”) with high affinity for NIR fluorochromes allows protein and cell specific labeling for *in vivo* imaging. *PLoS One* **2007**, *2* (7), e665.
- (25) Bachmann, B. J.; Low, K. B.; Taylor, A. L. Recalibrated linkage map of *Escherichia coli* K-12. *Bacteriol. Rev.* **1976**, *40* (1), 116–67.
- (26) Schneider, C. A.; Rasband, W. S.; Eliceiri, K. W. NIH Image to ImageJ: 25 years of image analysis. *Nat. Methods* **2012**, *9* (7), 671–5.
- (27) Ghosh, A.; Guo, J. C.; Brown, A. D.; Royston, E.; Wang, C. S.; Kofinas, P.; Culver, J. N. Virus-assembled flexible electrode–electrolyte interfaces for enhanced polymer-based battery applications. *J. Nanomater.* **2012**, *2012*, 795892.
- (28) Liu, Y.; Wang, H.; Huang, J.; Yang, J.; Liu, B.; Yang, P. Microchip-based ELISA strategy for the detection of low-level disease biomarker in serum. *Anal. Chim. Acta* **2009**, *650* (1), 77–82.
- (29) Turpen, T. H.; Reinal, S. J.; Charoenvit, Y.; Hoffman, S. L.; Fallarme, V.; Grill, L. K. Malarial epitopes expressed on the surface of recombinant tobacco mosaic virus. *Biotechnology (N Y)* **1995**, *13* (1), 53–7.
- (30) Petukhova, N. V.; Gasanova, T. V.; Stepanova, L. A.; Rusova, O. A.; Potapchuk, M. V.; Korotkov, A. V.; Skurat, E. V.; Tsyalova, L. M.; Kiselev, O. I.; Ivanov, P. A.; Atabekov, J. G. Immunogenicity and protective efficacy of candidate universal influenza A nanovaccines produced in plants by tobacco mosaic virus-based vectors. *Curr. Pharm. Des.* **2013**, No. PMID:23394564.
- (31) Wu, L.; Jiang, L.; Zhou, Z.; Fan, J.; Zhang, Q.; Zhu, H.; Han, Q.; Xu, Z. Expression of foot-and-mouth disease virus epitopes in tobacco by a tobacco mosaic virus-based vector. *Vaccine* **2003**, *21* (27–30), 4390–8.
- (32) Paschke, M. Phage display systems and their applications. *Appl. Microbiol. Biotechnol.* **2006**, *70* (1), 2–11.
- (33) Khan, A. S.; Thompson, R.; Cao, C.; Valdes, J. J. Selection and characterization of peptide mimotopes binding to ricin. *Biotechnol. Lett.* **2003**, *25* (19), 1671–5.
- (34) Samuelson, P.; Werner, H.; Svedberg, M.; Stahl, S. Staphylococcal surface display of metal-binding polyhistidyl peptides. *Appl. Environ. Microbiol.* **2000**, *66* (3), 1243–8.
- (35) Ide, T.; Baik, S. H.; Matsuba, T.; Harayama, S. Identification by the phage-display technique of peptides that bind to H7 flagellin of *Escherichia coli*. *Biosci. Biotechnol. Biochem.* **2003**, *67* (6), 1335–41.
- (36) Han, Z.; Su, G.; Huang, C. Screening and identification of receptor antagonist for shiga toxin from random peptides displayed on filamentous bacteriophages. *Sci. China, Ser. C: Life Sci.* **1999**, *42* (1), 43–9.
- (37) Soykut, E. A.; Dudak, F. C.; Boyaci, I. H. Selection of staphylococcal enterotoxin B (SEB)-binding peptide using phage display technology. *Biochem. Biophys. Res. Commun.* **2008**, *370* (1), 104–8.
- (38) Ma, H.; Zhou, B.; Kim, Y.; Janda, K. D. A cyclic peptide–polymer probe for the detection of *Clostridium botulinum* neurotoxin serotype A. *Toxicon* **2006**, *47* (8), 901–8.
- (39) Petrenko, V. A.; Vodyanoy, V. J. Phage display for detection of biological threat agents. *J. Microbiol. Methods* **2003**, *53* (2), 253–62.